Sustainability of gasification-based cogeneration with agri-food residues and heat recovery technologies: Techno-economic and life cycle analyses

Simin Anvari[a], Roque Aguado[a], David Vera[a], Francisco Jurado[a], Marc A. Rosen[b]

[a]Department of Electrical Engineering, University of Jaén, EPS Linares, Avda. de la Universidad s/n, 23700 Linares, Spain

[b]Faculty of Engineering and Applied Science, University of Ontario Institute of Technology, 2000 Simcoe Street North, Oshawa, Ontario, L1G 0C5, Canada

Abstract

For sustainable renewable energy, valorizing agri-food residues as biomass fuels through gasification and integrating heat recovery technology with gasifiers is important. Evaluating the environmental and economic aspects of energy systems requires both life cycle assessments (LCAs) and techno-economic analyses (TEAs). This study investigates the potential of three agri-food residues—almond hulls, exhausted olive pomace (EOP), and date palm fronds (DP) — as gasification biomass fuels. It then evaluates two heat recovery technologies: 1) a cleaning and cooling unit with an internal combustion engine (ICE) and a hot water production unit, and 2) an externally fired gas turbine combined with the organic Rankine cycle (EFGT_ORC) and a hot water production unit. It is shown that the EFGT_ORC cogeneration consistently requires lower biomass input than the ICE, with DP fronds leading in the ICE at 36 g/s, followed by almond hulls at 32 g/s, and EOP at 28 g/s. ICE cogeneration leads to some significant environmental impacts contributes to climate change, with emissions around 2.95×10^{-2} kg CO_2 eq. for all fuels. In terms of human health, DP fronds have a greater impact in EFGT_ORC cogeneration than in ICE. Almond hulls exhibit better economic performance, with higher values of NPV, PI, and IRR compared to EOP and DP fronds, even though biomass and electricity price variations significantly affect system sustainability, particularly for EOP.

Keywords: Biomass, Agri-food residue, Gasification technology, Waste heat recovery, Cogeneration, Bioenergy, Life cycle assessment, Techno-economic analysis

1 Introduction

The potential of agri-food value chain residues as biomass fuel for bioenergy production hinges on their abundant, renewable nature and their capacity to contribute to a circular economy [1, 2]. These residues—which include crop remnants, husks, shells, and agro-industrial by-products—possess considerable untapped energy potential. Effectively converting these residues into bioenergy can significantly reduce reliance on fossil fuels and decrease greenhouse gas emissions. Moreover, this approach addresses waste disposal challenges and provides a renewable source of energy [3]. This strategy is particularly important as global energy demands increase and the shift toward sustainable, low-carbon energy sources becomes increasingly necessary.

Gasification technology plays a pivotal role in transforming agricultural residues into bioenergy [4]. It is a thermochemical process that converts organic or fossil-based carbonaceous materials into carbon monoxide, hydrogen, and carbon dioxide at high temperatures in the presence of a controlled amount of oxygen and/or steam [5]. Unlike combustion, gasification breaks down the molecular structure of biomass residues into simpler molecules in the form of syngas (synthetic gas), which can then be used directly for heating or in internal combustion engines, or can be further processed into liquid biofuels, chemicals, or electricity. This technology is crucial for bioenergy production from agricultural residues because it can handle a variety of biomass types, including those with high moisture or ash content that are otherwise challenging to utilize [4]. Furthermore, gasification can achieve higher efficiencies and produce cleaner energy compared to direct combustion processes, making it a vital tool in the sustainable management and valorization of agricultural residues for energy production [6].

Utilizing syngas produced from biomass gasification in internal combustion engine (ICE) or organic Rankine cycle (ORC) systems offers efficient pathways to generate electricity and heating [7]. In ICEs, syngas replaces conventional fuels, converting its energy into mechanical energy and then electricity, leveraging existing engine technologies. The ORC, which is suited for low-grade heat, uses syngas to heat an organic fluid, driving a turbine to produce electricity at efficiencies higher than traditional steam cycles at similar temperatures. These approaches not only recycle waste into valuable energy, reducing environmental impact and enhancing energy diversity but also support a circular economy by efficiently harnessing renewable resources for power and heating [8]. Susastriawan et al. [9] conducted a thorough review of biomass gasification literature, focusing on its integration with internal combustion engines. They underscored the potential of biomass waste producer gas as a renewable fuel for both spark ignition (SI) and compression ignition (CI) engines. The review delved into various gasifier designs and operational factors affecting performance, including feedstock properties, gasification medium, equivalence ratio, and temperature. Tar removal methods, essential for engine fuel applications, were discussed, with an emphasis on achieving tar content below 100 mg/Nm^3. Rovas and Zabaniotou [10] performed an exergy analysis of a cogeneration system, a small gasification-based bioenergy setup fueled by Mediterranean agro-food processing wastes like olive kernel, fruit kernel, and wine production waste biomass. The system, designed for a maximum thermal output of 12 kW and about 5 kW of electrical output, includes a fluidized bed gasifier, a producer gas cooling/cleaning system, and an ICE. Varying exergy efficiency were obtained, based on feedstock, with olive kernel showing the highest efficiency, highlighting the impact of feedstock characteristics on system performance. Anvari et al. [11] introduced a system that combines a biomass gasification-powered gas turbine with an ORC and absorption cooling system for generating electricity and cooling. This research explores several steam injection methods aimed at improving efficiency and reducing CO_2 emissions. The study emphasizes the significance of using biomass as a renewable source for combined heat and power generation, presenting a viable strategy for enhancing energy efficiency and addressing environmental concerns. Gonzalez et al. [12] examined the thermodynamic performance of an integrated gasification-power plant (IGPP) in the sawmill industry, evaluating the potential of biomass gasification, utilizing pinewood chips residues, for combined heat and power generation. The findings suggest that the IGPP, in conjunction with heat recovery from exhaust gases, has the potential to furnish more than half of the electricity and nearly 40% of the thermal energy required for the sawmill process. Kavathia and Prajapati [13] explored the utilization of fruit and vegetable waste in biomass-fired combined heat and power systems, particularly focusing on their integration with regenerative organic Rankine cycle (RORC). The study emphasized the potential of anaerobic digestion as an effective waste treatment method, highlighting its ability to produce methane with minimal carbon emissions. Furthermore, it underscored the significance of organic working fluids in ORC systems, favoring dry fluids for their enhanced heat of vaporization. Additionally, the research examined various parameters influencing the economic viability of RORC systems and notes the availability of biomass-fired combined systems achieving electrical efficiency levels between 15% and 20%.

Life cycle assessment (LCA) and Techno-economic analysis (TEA) are useful tools in evaluating the environmental and economic viability of thermodynamic cycles, which are the heart of many energy systems, including power plants, refrigeration systems, and various industrial processes [14]. Performing an LCA allows engineers and researchers to evaluate the environmental effects across a system's entire lifecycle. In the context of thermodynamic cycles, an LCA measures the ecological impact, including greenhouse gas emissions, energy use, water consumption, and other environmental factors [15]. This process aids in steering the development of designs toward more eco-friendly options. In tandem, TEA provides a comprehensive evaluation of the economic aspects of these cycles, examining costs associated with development, implementation, operation, and maintenance, as well as potential revenues from the sale of energy or by-products [16]. It assesses the financial feasibility and competitiveness of different technologies or processes, considering factors like capital investment, operating costs, energy prices, and return on investment. Voultsos et al. [17] examined the energetic and environmental aspects of a cogeneration biomass gasification plant located in Thessaly, Greece, employing a combination of process simulation and LCA. Through simulations of the gasification process using various agricultural residues found in the region, they assessed the impact of technical parameters such as gasification temperature, equivalence ratio, and biomass moisture content, revealing a maximum gasification efficiency of approximately 70% across all feedstock types. When scaled up to a 1 MW_{el} and 2.25 MW_{th} cogeneration plant, the LCA highlighted electricity self-consumption as a significant contributor to both global warming potential (GWP) and non-renewable Fossil energy demand. Additionally, they quantified CO_2 mitigation and non-renewable energy savings, underscoring the environmental advantages of biomass cogeneration, although these are influenced by factors such as heat utilization and biomass availability. Chen et al. [18] investigated the thermodynamic and environmental performance of supercritical water gasification for hydrogen production, utilizing residue from a simultaneous saccharification and fermentation process with corn stover as the feedstock. By integrating waste heat recycling through the ORC and reheating cycle, energy efficiency improved by 5.7% and 9.2%, respectively. LCA conducted with SimaPro demonstrated the system's environmental friendliness, with GWP and acidification potential (AP) values indicating its superiority over alternative residue treatment technologies. Pati et al. [19] conducted an integrated analysis of a co-gasification-fermentation model for bio-ethanol production from Indian lignocellulosic biomass. Using Aspen Plus, the study assessed techno-economic and environmental aspects, revealing a minimum ethanol selling price of 0.65 $/L and reduced CO_2 emissions compared to traditional methods. Monte Carlo simulation yielded an 81.8% probability of a non-negative net present value (NPV), indicating favorable financial prospects. Furthermore, life cycle analysis demonstrated reduced CO_2 emissions compared to traditional ethanol production, with the co-gasification-fermentation process, yielding 1.23 kg less CO_2 per kg of bio-ethanol. Modifications to the model improved resource utilization and reduced environmental impact, highlighting its economic viability and environmental benefits. Chen et al. [20] conducted a thorough techno-economic assessment of a combined cooling, heating, and power system (CCHP) integrated with an ORC and absorption heat pump, driven by a natural gas-powered ICE. Aimed at enhancing energy efficiency and reducing emissions, the study employed a modified techno-economic method coupled with life cycle analysis to evaluate specific costs for electricity, cooling, and heating. It was seen that electricity is the least expensive commodity at 0.145 $/kWh, while cooling emerged as the priciest at 0.663 $/kWh. Emphasizing the importance of considering equivalent emissions in life cycle assessments, the research provided insights into the economic and environmental performance of integrated energy systems. Zang et al. [21] performed a study aimed at designing a CCHP system tailored to meet the energy needs of an office building at the University of Iowa in the U.S. By comparing six system options that varied in wood-tire mixture ratios and gasifier numbers, they employed Aspen Plus and MATLAB models to simulate the process. A discounted cash flow rate of return analysis was used to evaluate the levelized cost of electricity (LCOE), factoring in heating and cooling as byproducts. It was determined that a 100% wood gasification model with four gasifiers consistently achieved the highest average energy efficiency, ranging from 37% to 66%, while the 100% tire gasification model exhibited the lowest LCOE at 0.15 $/kWh. The study highlighted decarbonization potential and suggested future research areas: life cycle assessment, expanding to more buildings, and pilot-scale CHP system testing for enhanced efficiency.

Based on comprehensive studies, it becomes evident that harnessing agri-food residues as biomass fuels through gasification technology, integrated with ICE or ORC systems for electricity and heating production, represents an important step towards sustainable energy. The synergy of these technologies not only capitalizes on the renewable nature of agricultural waste, minimizing environmental impact and enhancing energy security, but also underscores the efficiency and versatility of bioenergy production pathways. Simultaneously, the application of LCA and TEA in evaluating these systems is important for ensuring environmental sustainability and economic viability, offering a holistic view of their impact and performance, thereby guiding optimization and policy-making towards greener energy futures. As a consequence, the objectives pursued in this article is to apply techno-economic and life cycle analyses to assess the sustainability of gasification-based cogeneration with agri-food residues and heat recovery technologies. The steps followed in the study follow:

- Examining the residues from three different agri-food value chains—almond hulls, exhausted olive pomace, and date palm fronds —as sources of biomass fuel with the highest potential for bioenergy in Tunisia.

- Investigating the gasification of all three considered biomass fuels in a downdraft gasifier under uniform gasification conditions.
- Energy recovery from the gasification unit for electricity and heating generation through two technologies involving: 1) integrating the cooling and cleaning unit with an internal combustion engine, and 2) integrating an externally fired gas turbine to the Rankine cycle.
- Implementing energy analysis for both simulated cogeneration systems across the three investigated biomass fuels: calculating mass balances, energy balances, and energy efficiencies.
- Conducting life cycle assessment analysis on both simulated cogeneration systems for each of the three studied fuels: midpoint and endpoint methods.
- Conducting techno-economic analysis: calculating net present value, simple and discounted payback periods, levelized cost of electricity and profitability index.

Thus, the main objective of this article is to conduct a comparative study of two proposed cogeneration systems using different fuels. Grounded in environmental and economic analysis, the comparison seeks to identify the most economically viable system while constraining or minimizing pollutant emissions. This study examines three distinct biomass fuels with both cogeneration systems to achieve its objectives.

2 Material and methods

In this section, an introduction is provided to the biomass fuels employed here for the gasification processes of the cogeneration systems. Then, the simulated cogeneration systems are presented, alongside the analytical tools and methodologies applied to these systems. This includes life cycle assessment and techno-economic analysis, which are discussed in detail.

2.1 Biomass fuels in the gasification processes

The importance and potential of agricultural product residue, as well as its significant potential for bioenergy production, were mentioned in the introduction section. The biomass potential can vary depending on the annual production of agricultural products in different countries [22]. In Tunisia, three agricultural products, namely olive, date palm, and almond, have the highest production rates. According to the prior work [22], exhausted olive pomace (EOP), date palm (DP) fronds, and almond hulls, with 5355 TJ, 4538 TJ, and 2766 TJ respectively, have the highest bioenergy production rates. Therefore, in this study, these three types of agricultural residue are used as fuels in the gasification process of the proposed cogeneration systems. Figure 1 shows these three types of agricultural residue.

Figure 1 Types of biomass fuels used in the gasification processes of the simulated cogeneration systems: a) almond hulls, b) EOP, and c) DP fronds.

2.2 Proposed cogeneration systems utilizing gasification technology

Figures 2 and 3 illustrate the cogeneration systems proposed in this study. The simulations of the systems are carried out using Thermoflex software, a comprehensive tool for modeling thermal systems. As observed, in both cogeneration systems, the gasification process is utilized for valorizing biomass fuels. This involves biomass reacting with air in a downdraft gasifier to produce hot syngas. However, to recover energy from the produced hot syngas, two methods are employed, which are detailed subsequently.

In Figure 2, an ICE is utilized for the recovery of energy from gasification. Initially, the hot syngas output from the gasifier is directed to the cooling and cleaning unit to generate cold syngas. Then, the cold syngas is fed into the internal combustion engine, which leads to electricity generation. In parallel, hot water is produced by capturing the energy from the jacket water cooling system employed for cooling the engine. In Figure 3, an external fired gas turbine (EFGT) equipped with heat exchanger 2 (HX2) and an ORC is utilized to recover energy from the hot syngas produced by the gasification unit. Initially, the hot syngas combusts in a combustion chamber with air supplied by an air compressor, generating hot gases. These hot gases then enter turbine 1, where they generate power. Following this, the expanded gases move into heat exchanger 1 (HX1) to transfer energy to thermal oil, supplying the necessary energy to drive the Rankine cycle. Note that, in this simulation, the energy from the hot gases is not directly used to power the ORC, to ensure the working fluid retains its physical properties [23]. The hot gases exiting HX1 are recuperated by HX2 and are used for hot water production. Furthermore, in the Rankine cycle, the working fluid, after absorbing heat in the evaporator, expands through turbine 2, generating power. The detailed assumptions made in the modeling of both cogeneration systems are specified in Table 1.

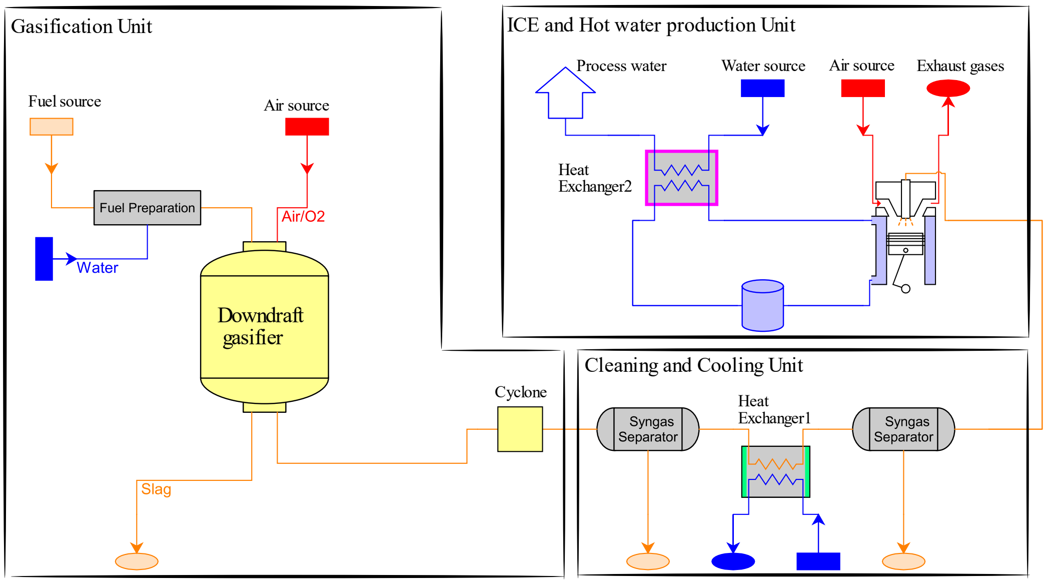

Figure 2 Modeled cogeneration system using an ICE

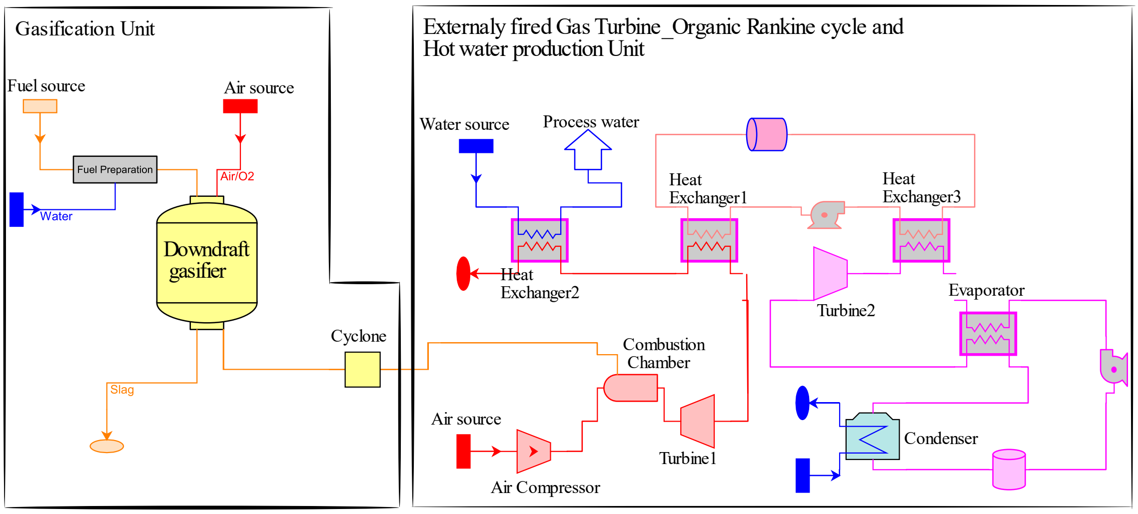

Figure 3 Modeled cogeneration system using an EFGT_ORC

Table 1 Assumptions for inputs and outputs in the modeled cogeneration systems

Parameter	Value
Ambient air pressure and temperature	P_0=1.013 bar, T_0= 20 ^{0}C
Gasification pressure and temperature	$P_{gasifier}$=1.013 bar, $T_{gasifier}$= 850 ^{0}C
Exit temperature of cyclone	$T_{cyclone}$= 400 ^{0}C
Pressure drop at gas side of heat exchangers	0.1 bar
Pinch point temperature of HX1, HX2 and evaporator	$\Delta T_{HX1}=\Delta T_{HX2}=\Delta T_{Eva}$=2.78^{0}C
Pressure drop correction factor at separators	0.1 bar

Heat rejection per unit of inlet syngas at separators	10 kJ/kg
Fuel inlet pressure and temperature to engine	P_0=1.012 bar, T_0= 35 ^{0}C
Exhaust gas temperature of engine	$T_{Exhaustgas}$= 515 ^{0}C
Inlet air pressure and temperature to engine	P_{air}=1.013 bar, T_{air}= 20 ^{0}C
Output temperature of combustor	950 ^{0}C
Pressure ratio of air compressor and gas turbine	12 bar
Mechanical efficiency of air-compressor and gas turbine	99.8%
Organic working fluid in ORC	Toluene
Design point pressure of turbine	25 bar
Mechanical efficiency of turbine	99.75%
Mass flow rate of water input to condenser	3 kg/s

Descriptions related to the biomass gasification process in the gasifier, as well as the governing equations for biomass combustion with air, are provided in Reference [24]. The energy efficiencies for the cogeneration system equipped with an ICE and for the cogeneration system utilizing the EFGT_ORC are calculated as follows:

$$\eta_{CHP,ICE} = \frac{P_{gen,ICE} + \dot{Q}_{th,ICE}}{\dot{Q}_{in}} \quad (1)$$

$$\eta_{CHP,EFGT\_ORC} = \frac{P_{gen,GT} + P_{gen,ORC} + \dot{Q}_{th,HX2}}{\dot{Q}_{in}} \quad (2)$$

Here, $\dot{Q}_{in}$ denotes the input energy rate to the systems through biomass gasification [24]; $P_{gen,ICE}$ and $\dot{Q}_{th,ICE}$ are the generated electricity and hot water rates by the ICE, respectively, the corresponding equations for which are detailed in Reference [24]. The net produced electricity rate by the EFGT is denoted by $P_{gen,GT}$, while $P_{gen,ORC}$ is the net generated electricity rate through the Rankine cycle, and $\dot{Q}_{th,HX2}$ indicates the hot water production rate by HX2. These parameters can be expressed as follows:

$$P_{gen,GT} = \dot{W}_{Turbine1} - \dot{W}_{AirCompressor} \quad (3)$$

$$P_{gen,ORC} = \dot{m}_{ORC}\left[\left(h_{in,turbine2} - h_{out,turbine2}\right) - \left(h_{out,pump} - h_{in,pump}\right)\right] \quad (4)$$

$$\dot{Q}_{th,HX2} = \dot{m}_{water}\left(h_{out,HX2} - h_{in,HX2}\right) \quad (5)$$

3 Life cycle assessment methodology

The life cycle assessment method offers a comprehensive perspective on the environmental aspects of products or systems, enabling a thorough evaluation of their overall environmental impacts. This approach examines the impacts of energy inputs and waste outputs on the environment, covering effects on air, water, land, and human health. Through LCA, businesses, policymakers, and consumers can make informed decisions, grounded in a thorough understanding of the environmental implications of products and services. This fosters a move towards sustainability and the minimization of environmental footprints. The methodology unfolds across four main stages: defining the goal and scope, inventory analysis, impact assessment, and interpretation [25]. Each stage is detailed further below.

3.1 Goals and Scope Definition

The initial stage of LCA consists of establishing the study's objectives and scope, determining the functional unit, setting the system boundaries, and outlining the study's assumptions. This study aims to evaluate the environmental performance of electricity production from valorization of different biomass fuels, including almond hulls, EOP, and DP fronds, using gasification technology. It involves a comparison between two cogeneration systems: one utilizing gasification coupled with an ICE and the other employing gasification followed by an EFGT and an ORC. The simulated cogeneration systems produce both electricity and heat energies; however, for the LCA analysis, the functional unit (FU) is specified as the production of 100 kJ of electricity. The LCA adhered to a gate-to-cradle boundary approach, focusing on the conversion of biomass fuels into energy. In the other world, this study does not account for downstream activities, including the extraction of olive oil, production of date fronds, almond hulls production, and the potential transportation of residues from these agricultural products.

The rationale behind this exclusion is the assumption that the impacts or metrics related to these processes remain consistent across all management options evaluated [26].

In this article, a simulation of gasification for three specified biomass types in two cogeneration systems is presented, leading to a comparison across six different scenarios for generating electricity. To ensure the comparability of the outcomes from these six scenarios, analyses of mass and energy for each cogeneration system are carried out under a consistent set of assumptions. These assumptions include maintaining the same temperature and pressure in the gasifier, as well as identical cyclone outlet temperatures for all three types of fuel. Additionally, when conducting the LCA analysis, the assessment does not consider capital goods like machinery, equipment, and buildings.

3.2 Life cycle inventory analysis

Life Cycle Inventory (LCI) analysis involves data collection and calculation procedures to quantify relevant inputs and outputs of a product system [27]. Inputs include raw materials, energy use, and other resources, while outputs involve emissions to air and water, solid waste, and various environmental discharges. This phase aims to compile an inventory of all relevant energy and material inputs and environmental releases associated with the product system [27]. As previously stated, the evaluated cogeneration systems, fueled by various types of biomass, were modeled using Thermoflex software to calculate their mass and energy balances. Consequently, these simulations yielded valuable insights into emissions, resource utilization, and energy consumption for each case. The LCI data for both proposed cogeneration systems, utilizing different biomass fuels, are detailed in Tables 2 and 3.

Table 2 Data on inventory for the cogeneration system modeled with an ICE, differentiated by biomass fuel types, based on FU=100 kJ of electricity production.

Stage	Inputs/outputs	Almond (hulls)	EOP	DP (fronds)
Gasification unit	Biomass (g)	31.9	28.3	36.6
	Air (g)	52.3	58	41.4
	Gasifying agent (kJ)	1.675	1.664	1.69
	Heat losses (kJ)	55.13	56.22	53.59
	Slag (g) (ash/carbon/chlorine)	0.8	0.4	1.3
Cleaning and cooling unit	Emissions to air (g)			
	H_2O	6.37	5.74	8.31
	CO	2.23	2.26	2.026
	H_2S	0.003	0.024	0.15
	COS	0.00014	0.0008	0.004
	Ar	0.51	0.57	0.4
ICE and hot water production unit	Emissions to air (g)			
	N_2	117.3	121.74	108.81
	O_2	0.0223	0.026	0.0305
	CO_2	29.6	28.82	28.42
	H_2O	22.3	22.12	24.32
	Ar	0.91	0.91	0.914

Table 3 Data on inventory for the cogeneration system modeled with an EFGT_ORC, differentiated by biomass fuel types, based on FU=100 kJ of electricity production.

Stage	Inputs/outputs	Almond (hulls)	EOP	DP (fronds)
Gasification unit	Biomass (g)	17.9	16	21.1
	Air (g)	29.8	34	25
	Gasifying agent (kJ)	1.64	1.632	1.65
	Heat losses (kJ)	33.22	33.75	33.43
	Slag (g) (ash/carbon/chlorine)	0.3	0.2	0.8
EFGT_ORC, and hot water production unit	Electricity consumption (kJ)	0.8296	0.8297	0.8296
	Emissions to air (g)			
	N_2	235	235	232
	O_2	45	44.2	45
	CO_2	12	17	17.35
	H_2O	21	21	24.5
	Ar	2.8	2.83	2.8
	SO_2	0.0035	0.03	0.19

3.3 Impact assessment methodology

In the present investigation, the LCA is executed employing SimaPro software, which conforms to the standards established by the International Organization for Standardization (ISO), specifically those delineated in ISO 14040 and 14044 [28]. With LCA, the impact assessment stage is important as it interprets the inventory of material inputs and environmental releases to assess their potential impacts on the environment and human health. The impact assessment phase often involves two methods: mid-point and end-point [29]. Mid-point methods are characterized by their focus on immediate environmental impacts, such as global warming or acidification [30]. They deliver detailed and scientifically reliable insights with a high degree of specificity. However, these methods necessitate further interpretation to fully grasp their implications in real-world scenarios. Conversely, end-point methods are designed to quantify the ultimate impacts on human health, ecosystems, and natural resources [30]. They yield intuitive, aggregated outcomes that facilitate decision-making processes, albeit at the risk of introducing greater uncertainty and the potential for oversimplification. Each approach caters to distinct analytical needs: mid-point methods provide in-depth understanding of specific environmental challenges, whereas end-point methods offer a streamlined overview of the ultimate consequences, enhancing decision-making at a broader level.

In this work, both approaches are utilized in conducting the LCA to leverage the advantages of each method, thereby providing a more comprehensive assessment of environmental impacts. Moreover, the results of all the impact scores are normalized, making them easier to compare between the impact categories. Normalization makes it easier to pinpoint which impact categories contribute most and least to environmental impacts, streamlining the decision-making process. The normalized environmental impacts are determined by dividing the environmental impacts of each category by a reference value, as follows [31]:

$$N_k = \frac{S_k}{R_k} \tag{6}$$

where k represents the category of impact, N is the environmental impact once normalized, S indicates the impact category's indicator from the characterization phase, and R is the normalization factor or reference value.

Finally, it is important to note that, in all cases examined, electricity production is the main output, with hot water production considered a by-product. Consequently, the environmental impacts of producing electricity and hot water in the cogeneration systems are allocated based on economic considerations. The environmental impacts of each process are allocated to the primary product in proportion to their total economic value, as follows [31]:

$$EA = \frac{EV \times M}{\sum_n (EV_n \times M_n)} \times 100 \qquad (7)$$

where EA represents the economic allocation as a percentage, EV denotes the economic value in \$/kWh, and M is the energy produced by each output, measured in kWh.

4 Techno-economic analysis

A comparative economic feasibility assessment of the proposed cogeneration plants with ICE and EFGT-ORC was performed in accordance with the standard methods for the financial appraisal of investments. These methods consider net present value, internal rate of return, payback period and levelized cost of electricity [32].

The net present value (NPV) provides the cumulative net cash flow discounted over the operational lifespan of the cogeneration plant to future value [32]. This parameter indicates the earnings after paying back the initial capital investment (INV). Therefore, NPV > 0 and NPV < 0 represent earnings and losses, respectively. NPV can be expressed as

$$\mathrm{NPV} = -\mathrm{INV} + \sum_{t=1}^{n} \mathrm{NCF}\,(1+i)^{-n} \tag{8}$$

where n is the total number of annual periods that make up the operational lifespan of the integrated gasification plant, *i* is the discount rate (real rate of interest) and NCF is the net cash flow in each period.

The internal rate of return (IRR) is the discount rate for which the NPV is equal to zero [33]. This parameter represents the maximum discount rate at which the investment breaks even. Calculation of the IRR can be performed iteratively by variation of the discount rate using the Newton–Raphson method.

Another key economic parameter is the profitability index (PI) [34], defined as the ratio of the net present value to the initial investment. A value greater than 1 indicates a profitable project. PI can be expressed as

$$\mathrm{PI} = \frac{\mathrm{NPV}}{\mathrm{INV}} \tag{9}$$

The simple payback period (SPB) is the period required to pay off the initial capital investment without accounting for the annual discount rate. It can be expressed by dividing the initial investment by the annual net cash flow:

$$SPB = \frac{\mathrm{INV}}{\mathrm{NCF}} \tag{10}$$

However, the discounted payback period is often used as an improved version of the SPB to better account for the present value of future cash flows. The DPB calculates the period after which an investment is expected to break even and, thus, it is consistent with the NPV. But NPV is more complex, leaving SPB as a commonly used financial indicator. The DPB can be calculated, assuming that each cash flow is equal, as follows (for constant cash flows):

$$\mathrm{DPB} = \frac{\log\left(\frac{1}{1 - \mathrm{INV}\,\frac{i}{\mathrm{NCF}}}\right)}{\log(1+i)} \quad (11)$$

The levelized cost of electricity (LCOE) indicates the minimum price at which electricity must be sold for the investment to break even [32]. The LCOE is measured in terms of cost per unit energy. This parameter is calculated as the ratio of the net present value of total capital and operating costs to the total electricity generation over the operational lifespan of the cogeneration plant, as follows:

$$\mathrm{LCOE} = \frac{\mathrm{INV} + \sum_{t=1}^{n} C_n\,(1+i)^{-n}}{\sum_{t=1}^{n} E_n\,(1+i)^{-n}} \quad (12)$$

where C_n and E_n respectively are the net cost (operation and maintenance cost and feedstock cost) and the electricity generation in each period.

5 Results and discussion

5.1 Almond (hulls), EOP and DP (fronds) characterization

As previously mentioned, the gasification process of the cogeneration systems examined in this paper employs three types of agri-food residues: almond hulls, EOP, and DP fronds. The results obtained from the ultimate and proximate analyses for these fuels are listed in Table 4, which also includes results for these fuel types from other research. As can be observed in this table, almond hulls, with 8% moisture content, have the highest level of moisture. Date palm fronds are next with 7.9%, followed by EOP with 6%. Almond hulls contain 5.7% ash, while date palm fronds contain 5.3% and EOP 4.6%. EOP has the highest higher heating value at 20 MJ/kg, followed by almond hulls and date palm fronds at 18.4 and 16.2 MJ/kg, respectively.

In Table 5, the specifications of the cold syngas fed to the ICE in the simulated cogeneration system equipped with an ICE are provided for each of the three biomass fuels studied. It is observed that the cold syngas produced in the cogeneration system through the gasification of date palm fronds fuel has the highest lower heating value at 5.46 kJ/kg. The cold syngas using almond hulls and EOP exhibit lower heating values of 4.84 and 4.6 kJ/kg, respectively.

Table 4 Heating value (higher/lower) and proximate and ultimate analyses of various samples of almond hulls, EOP, and DP fronds, on a dry basis.

Analysis/ Sample		**Almond (hulls)**			**EOP**			**DP (fronds)**		
		[35]	[36]	This work	[37]	[38]	This work	[39]	[40]	This work
Elemental analysis (wt %)	Moisture	6.72 ± 2.87	7.20	8.2	4.8-13.8	6.8	6.08	8.20 ± 0.72	8.50 ± 1.9	7.9
	Fixed carbon	18.77 ± 0.57	22.89	22.79	16.43-22.36	21.6	20.38	10.97 ± 1.00	9.12	11.6
	Volatile matter	62.72 ± 1.93	71.33	69	70.24-76.67	67.20	72	81.24 ± 2.64	72.28 ± 3.4	80
	Ash content	11.80 ± 0.37	5.78	5.7	5.4-9.2	4.4	4.6	7.67 ± 1.05	5.50 ± 0.7	5.3
Ultimate analysis (wt %)	C	44.23 ± 1.38	45.79	45.42	47.49-55.44	53.4	49.15	37.7 ± 1.31	39.95 ± 0.09	38
	H	4.65 ± 0.21	5.36	5.36	5.26-6.5	7.5	6.52	5.58 ± 0.17	7.19 ± 0.03	5.75
	O	49.88 ± 1.52	40.60	40.03	31.04-38.86	37.4	36.23	48.66 ± 1.96	52.70	46.7
	N	1.25 ± 0.07	0.96	0.96	0.40-2.20	1.7	0.8	1.35 ± 0.10	0.158 ± 0.03	1.16
	S	-	0.01	0.01	0.07-0.24	-	0.1	0.53 ± 0.02	-	0.48
Heating value (MJ/kg)	HHV	15.74 ± 0.50	18.22	18.38	19.12-20.94	20.70	20.452	-	19.09	16.2
	LHV	-	17.13	17.05	17.68-19.55	-	18.99	-	-	14.819

Table 5 Properties of the cold syngas input to the internal combustion engine of the ICE cogeneration cycle.

	Cogeneration with ICE		
Sample	**Almond (hulls)**	**EOP**	**DP (fronds)**
H_2 (%)	22.74	21.65	27.24
N_2 (%)	45.11	48.31	39.06
CO (%)	21.29	20.53	21
CO_2 (%)	10.86	9.507	12.69
CH_4 (%)	0.0039	0.0039	0.0043
Molecular weight (-)	23.84	23.9	22.96
LHV (kJ/kg)	4840	4626	5464
HHV (kJ/kg)	5260	5025	5986

5.2 Mass and energy balances of simulated cogeneration processes for various biomass fuels

To accurately understand the mass flows in simulated cogeneration systems, mass balances for these systems using almond hulls, EOP and DP fronds fuels, aimed at generating 100 kJ of electricity, are detailed (see Table 6). This table includes both the input and output masses of the cogeneration systems, presented in g/s and as percentages of the total input and output mass. Broadly, the data reveal that, for all three types of biomass fuel, the total mass input into the cogeneration equipped with EFGT_ORC is greater compared to the cogeneration equipped with ICE. Nonetheless, the biomass mass input into the EFGT_ORC cogeneration system is lower than that into the ICE cogeneration system for each fuel type. In the ICE cogeneration system, DP fronds allocate the highest biomass input mass to the gasifier at 36 g/s, followed by almond hulls at 32 g/s, and EOP at 28 g/s. Furthermore, among the output masses from the ICE cogeneration cycle, EOP contribute to 95% of the total mass exiting the cycle as exhaust gases from the engine, marking a higher percentage of exhaust gases from the internal combustion engine compared to DP fronds and almond hulls.

Table 6 Mass balances for simulated cogeneration with ICE and EFGT_ORC systems

	Cogeneration with ICE			Cogeneration with EFGT_ORC		
	Almond (hulls)	EOP	DP (fronds)	Almond (hulls)	EOP	DP (fronds)
$\dot{m}_{in}$ (g/s)	180.1 (100%)	182.1 (100%)	174.7 (100%)	321.9 (100%)	320 (100%)	322.1 (100%)
Biomass	31.9 (17.7%)	28.3 (15.5%)	36.6 (20.9%)	17.9 (5.56%)	16.1 (5%)	21.1 (6.6%)
Air into gasifier	52.3 (29%)	58 (31.8%)	41.4 (23.7%)	29.8 (9%)	34 (10.6%)	25 (7.7%)
Air into ICE	95.9 (53.2%)	95.8 (52.6%)	96.7 (55.3%)	274.2 (85.2%)	271 (84.7%)	276 (85.7%)
$\dot{m}_{out}$ (g/s)	180.1 (100%)	182.1 (100%)	174.7 (100%)	321.9 (100%)	320 (100%)	322.1 (100%)
Exhaust gases	170.2 (94.5%)	174 (95.3%)	162.5 (93.02%)	321.6 (99.9%)	319.7 (99.9%)	321.3 (99.7%)
Losses	9.9 (5.5%)	8.5 (4.7%)	12.2 (6.90%)	0.3 (0.09%)	0.2 (0.09%)	0.8 (0.25%)

Table 7 Energy balances in simulated cogeneration with ICE and EFGT_ORC systems

	Cogeneration with ICE			Cogeneration with EFGT_ORC		
	Almond (hulls)	EOP	DP (fronds)	Almond (hulls)	EOP	DP (fronds)
$\dot{E}_{in}$ (kW)	491.5 (100%)	485.3 (100%)	490.4 (100%)	277 (100%)	276 (100%)	284.6 (100%)
$\dot{E}_{out}$ (kW)						
Electricity production	100 (20.35%)	100 (20.6%)	100 (20.4%)	100 (36.1%)	100 (36.2%)	100 (35.2%)
Hot water production	122.8 (25%)	122.8 (25.3%)	122.8 (25%)	30.5 (11%)	28.7 (10.4%)	31.3 (11%)
Losses in gasification unit	71.75 (14.6%)	63.18 (13%)	71.2 (14.5%)	37.6 (13.6%)	37.7 (13.7%)	43.7 (15.3%)
Losses in cooling and cleaning unit	62.2 (12.65%)	63.6 (13.1%)	61.5 (12.5%)	-	-	-
Losses in ICE and hot water production unit	134.9 (27.44%)	135.7 (27.9%)	135.5 (27.6%)	-	-	-
Losses in EFGT_ORC, and hot water production unit	-	-	-	109.3 (39.5%)	109.1 (39.6%)	109.4 (38.4%)

Energy balances for cogeneration systems utilizing almond hulls, EOP, and DP fronds as fuels, with the objective of producing 100 kJ of electricity, are detailed in Table 7. In this table, the energy outputs from the cogeneration systems are expressed both in kW and as a percentage of the total energy input. It is generally observed that, for all fuels used, the total energy input into the cogeneration cycle utilizing ICE is roughly 43% higher than that for cycle employing EFGT_ORC. As a result, the amount of hot water generated in the cogeneration cycle with the ICE surpasses that of the EFGT_ORC cycle by approximately 75%.

The energy balance in the cogeneration cycle with an ICE exhibited similar behavior across all three fuels used in the gasifier. In this cycle, for each gasified fuel, 100 kJ of electricity (approximately 20% of the total input energy) and 112.8 kJ of hot water (approximately 25% of the total input energy) are produced. The largest energy loss is observed in the ICE and hot water production unit, accounting for about 27% of the total input energy. In the cogeneration cycle employing EFGT_ORC, approximately 36% of the input energy is allocated to electricity generation, and about 11% is utilized for hot water production across all three fuels. The EFGT_ORC unit records the highest energy losses for fuels such as almond hulls, EOPs, and DP fronds, with each fuel contributing to 38.5% of the total energy output as losses.

Ultimately, energy efficiencies for the cogeneration cycle using an ICE are determined to be 48.6%, 48.5%, and 48.7% for almond hulls, EOP, and DP fronds fuels, respectively. Similarly, for the EFGT_ORC cogeneration cycle, energy efficiency has been calculated at 47.8%, 47.7%, and 48.4% for almond hulls, EOP, and DP fronds fuels, respectively.

5.3 Life cycle assessment impact analysis

The results from the LCA analysis for both environmental methods, including midpoint and endpoint, are presented. It is noted that in the midpoint analysis, the examined parameters are as follows [41]:

- Climate change (CC): The emission of greenhouse gases such as carbon dioxide, methane, and nitrous oxide, contributing to global warming and climate change.
- Ozone depletion (OD): The release of substances like chlorofluorocarbons (CFCs) that deplete the ozone layer, resulting in increased ultraviolet radiation reaching the Earth's surface.
- Terrestrial acidification (TA): Signifying the release of acidic substances into terrestrial ecosystems, leading to soil and water acidification.
- Freshwater eutrophication (FE): Excessive nutrient enrichment of freshwater bodies, causing algal blooms and ecosystem degradation.
- Marine eutrophication (ME): Similar to freshwater eutrophication, but occurring in marine ecosystems.
- Human toxicity (HT): Referring to the potential harm posed to human health by exposure to toxic substances.
- Particulate matter Formation (PMF): The generation of fine particles in the atmosphere, which can adversely affect both human health and the environment.
- Natural land and fossil depletion (FD): Encompassing the depletion of natural resources, including both renewable (e.g., forests) and non-renewable (e.g., fossil fuels) resources.

In the endpoint analysis, the examined parameters are [41]:

- Human health (HH): Reflecting the overall impact on human health resulting from the environmental stressors assessed in the midpoint analysis.

- Ecosystem diversity (ED): Representing the diversity and integrity of ecosystems, encompassing species richness and habitat quality.
- Resource availability (RA): Indicating the availability of resources necessary for sustaining human activities and ecosystems, including water, minerals, and energy sources.

In Table 8, the LCA analysis results using the midpoint method for both proposed cogeneration systems and all three fuels are listed. It is evident that, for each fuel, cogeneration utilizing the ICE significantly impacts climate change when compared to the system based on EFGT_ORC. Specifically, the ICE cogeneration system powered by almond hulls, EOP, and DP fronds fuels demonstrate environmental climate change impacts of 2.99×10^{-2}, 2.91×10^{-2}, and 2.88×10^{-2} kg CO_2 eq, respectively. In contrast, the EFGT_ORC cogeneration system accounts for about 4.75×10^{-4} kg CO_2 eq of the climate change impacts for each of these fuels. Regarding ozone depletion, terrestrial acidification, freshwater eutrophication, marine eutrophication, particulate matter formation, and natural land and fossil depletion, the analysis indicates that for all three fuels utilized in the gasification process, the EFGT_ORC cogeneration exhibits greater environmental impacts than the ICE cogeneration cycle. Notably, TA and PMF effects in the EFGT_ORC cogeneration with DP fronds fuel represent 84% of the total impacts for these categories, in comparison to other fuels in this cycle. Additionally, the human toxicity impact in the ICE cogeneration cycle (2.41×10^{-4} kg 1,4-DCB for almond hulls, 1.59×10^{-4} kg 1,4-DCB for EOP, and 3.43×10^{-4} kg 1,4-DCB for DP fronds) exceeds that of the EFGT_ORC cogeneration (1.76×10^{-4} kg 1,4-DCB for almond hulls, 1.55×10^{-4} kg 1,4-DCB for EOP, and 2.78×10^{-4} kg 1,4-DCB for DP fronds), with the most significant human toxicity impact observed for DP fronds fuel in the ICE cogeneration cycle.

Table 8 Comparison of environmental impacts of cogeneration systems for various fuels, based on midpoint analysis

Environmental impact/value	Cogeneration with ICE			Cogeneration with EFGT_ORC		
	Almond (hulls)	**EOP**	**DP (fronds)**	**Almond (hulls)**	**EOP**	**DP (fronds)**
Climate change (kg CO_2 eq)	2.99×10^{-2}	2.91×10^{-2}	2.88×10^{-2}	4.70×10^{-4}	4.66×10^{-4}	4.87×10^{-4}
Ozone depletion (kg CFC11 eq)	1.29×10^{-10}	1.23×10^{-10}	1.36×10^{-10}	1.80×10^{-10}	1.78×10^{-10}	1.86×10^{-10}
Terrestrial acidification (kg SO_2 eq)	3.29×10^{-7}	2.69×10^{-7}	4.04×10^{-7}	3.86×10^{-6}	3.03×10^{-5}	1.90×10^{-4}
Freshwater eutrophication (kg P eq)	2.25×10^{-8}	1.79×10^{-8}	2.83×10^{-8}	2.32×10^{-8}	2.20×10^{-8}	2.89×10^{-8}
Marine eutrophication (kg N eq)	1.40×10^{-9}	1.11×10^{-9}	1.77×10^{-9}	1.43×10^{-9}	1.35×10^{-9}	1.79×10^{-9}
Human toxicity (kg 1,4-DCB)	2.41×10^{-4}	1.59×10^{-4}	3.43×10^{-4}	1.76×10^{-4}	1.55×10^{-4}	2.78×10^{-4}
Particulate matter formation (kg PM2.5 eq)	1.33×10^{-7}	1.05×10^{-7}	1.68×10^{-7}	1.15×10^{-6}	8.83×10^{-6}	5.53×10^{-5}
Natural land and fossil fuel depletion (kg oil eq)	1.38×10^{-4}	1.33×10^{-4}	1.44×10^{-4}	1.95×10^{-4}	1.93×10^{-4}	2.00×10^{-4}

The LCA analysis results using the endpoint approach are listed in Table 9. When assessing the environmental impact on human health, the ICE cogeneration system demonstrates notable effects, showing a 2.75×10^{-8} impact for both almond hulls and EOP. In contrast, the EFGT_ORC cogeneration system showed a 1.22×10^{-9} impact for almond hulls and a 6.03×10^{-9} impact for EOP. However, utilizing DP fronds fuel resulted in a higher impact on human health in the EFGT_ORC cogeneration cycle, at 3.52×10^{-8}, compared to 2.69×10^{-8} in the ICE cogeneration system. For ecosystem diversity impacts, the ICE cogeneration system accounted for 8.40×10-^{11}, 8.17×10^{-11}, and 8.08×10^{-11} respectively for almond hulls, EOP, and DP fronds fuels. In contrast, the EFGT_ORC cogeneration system recorded impacts of 2.25×10^{-12}, 7.85×10^{-12}, and 4.19×10^{-11} for the same fuels respectively. Regarding resource availability impacts, almond hulls, EOP, and DP fronds fuels in the EFGT_ORC cogeneration cycle contributed to 19%, 19%, and 20% of the total impacts respectively, while in the ICE cogeneration cycle, the impacts were 14%, 13%, and 14% respectively.

Table 9 Comparison of environmental impacts of cogeneration systems for various fuels, based on endpoint analysis

Environmental impact/value	Cogeneration with ICE			Cogeneration with EFGT_ORC		
	Almond (hulls)	EOP	DP (fronds)	Almond (hulls)	EOP	DP (fronds)
Human health	2.79×10^{-8}	2.72×10^{-8}	2.69×10^{-8}	1.22×10^{-9}	6.03×10^{-9}	3.52×10^{-8}
Ecosystems	8.40×10^{-11}	8.17×10^{-11}	8.08×10^{-11}	2.25×10^{-12}	7.85×10^{-12}	4.19×10^{-11}
Resources available	4.92×10^{-5}	4.77×10^{-5}	5.12×10^{-5}	6.99×10^{-5}	6.93×10^{-5}	7.17×10^{-5}

The results of the environmental impact assessments, normalized through midpoint analysis for various fuels utilized in both the ICE and EFGT_ORC cogeneration systems, are depicted in Figure 4. It is evident that the impacts on climate change for all three fuel types are markedly greater in the ICE cogeneration cycle compared to the EFGT_ORC cogeneration cycle. For all three fuels, the EFGT_ORC cogeneration cycle exhibits higher environmental impacts in terms of TA, PMF, and FD than the ICE cogeneration cycle. Note that the employment of DP fronds as fuel presents the most substantial environmental impacts when compared with almond hulls and EOP fuels in EFGT_ORC cogeneration cycle.

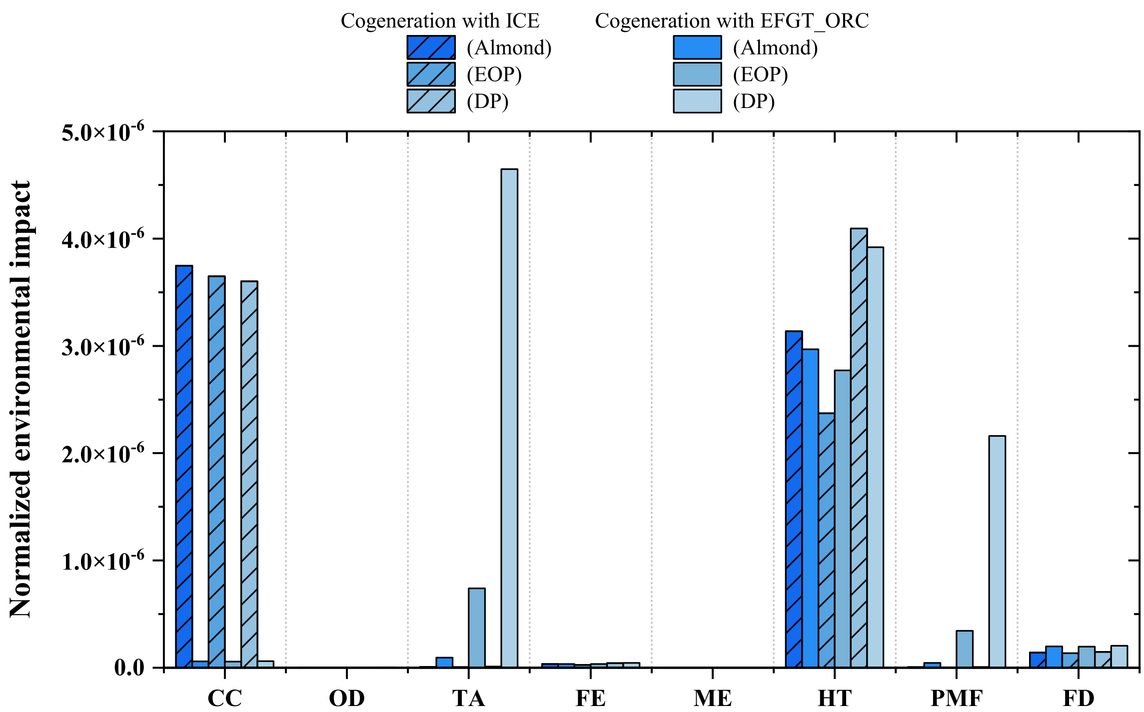

Figure 4 Normalized environmental impact of cogeneration systems for various fuels, based on midpoint analysis

The normalized environmental impacts assessed using endpoint analysis for various fuels employed in the simulated cogeneration systems are illustrated in Figure 5. It is observed that the use of almond hulls and EOP in the ICE cogeneration cycle results in higher impacts on human health and ecosystems compared to the EFGT_ORC cogeneration system. Notably, the EFGT_ORC cogeneration system demonstrates a distinct outcome for the impact on human health when using DP fronds, showing that this impact is more significant than that of the ICE cogeneration system. Contrary to the previous effects, the environmental impacts of using almond hulls, EOP, and DP fronds fuels in the ICE cogeneration cycle are less significant in terms of resource depletion compared to those in the EFGT_ORC cogeneration system.

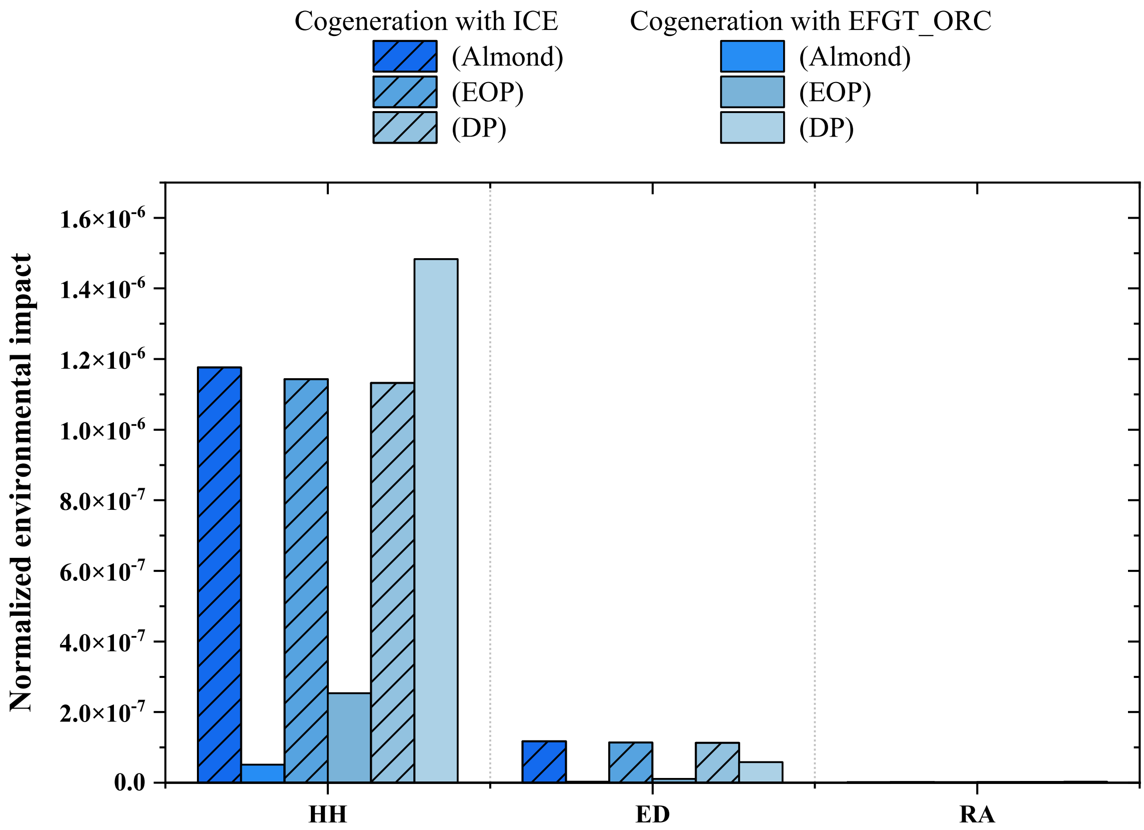

Figure 5 Normalized environmental impact of cogeneration systems for various fuels, based on endpoint analysis

Table 10 presents the results of the economic allocation for electricity, generated as the main product, and for hot water, produced as a by-product, across various fuels in the simulated cogeneration systems. As observed, the EFGT_ORC cogeneration system, due to its lower hot water output compared to the ICE cogeneration system, allocates a larger economic share to the generated electricity.

Table 10 Economic allocation value to various products of the cogeneration systems, 1) CHP_ICE (cogeneration with ICE), and 2) CHP_ORC (cogeneration with EFGT_ORC), categorized by biomass fuel type

Output	Economic value [42-44]	Almond (hulls)		EOP		DP (fronds)	
		CHP_ICE	CHP_ORC	CHP_ICE	CHP_ORC	CHP_ICE	CHP_ORC
Electricity	0.1 $/kWh	89.06%	97.03%	89.06%	97.20%	89.06%	96.96%
Hot water	0.01 $/kWh	10.94%	2.97%	10.94%	2.8%	10.94%	3.04%

Finally, the developed midpoint environmental impacts for the ICE cogeneration system in comparison with the EFGT_ORC cogeneration system for the considered biomass fuels, are illustrated in Figure 6. It is evident, apart from human toxicity and climate change impacts, that the remaining midpoint impacts demonstrate a decrease in environmental effects for the ICE cogeneration system relative to the EFGT_ORC cogeneration system.

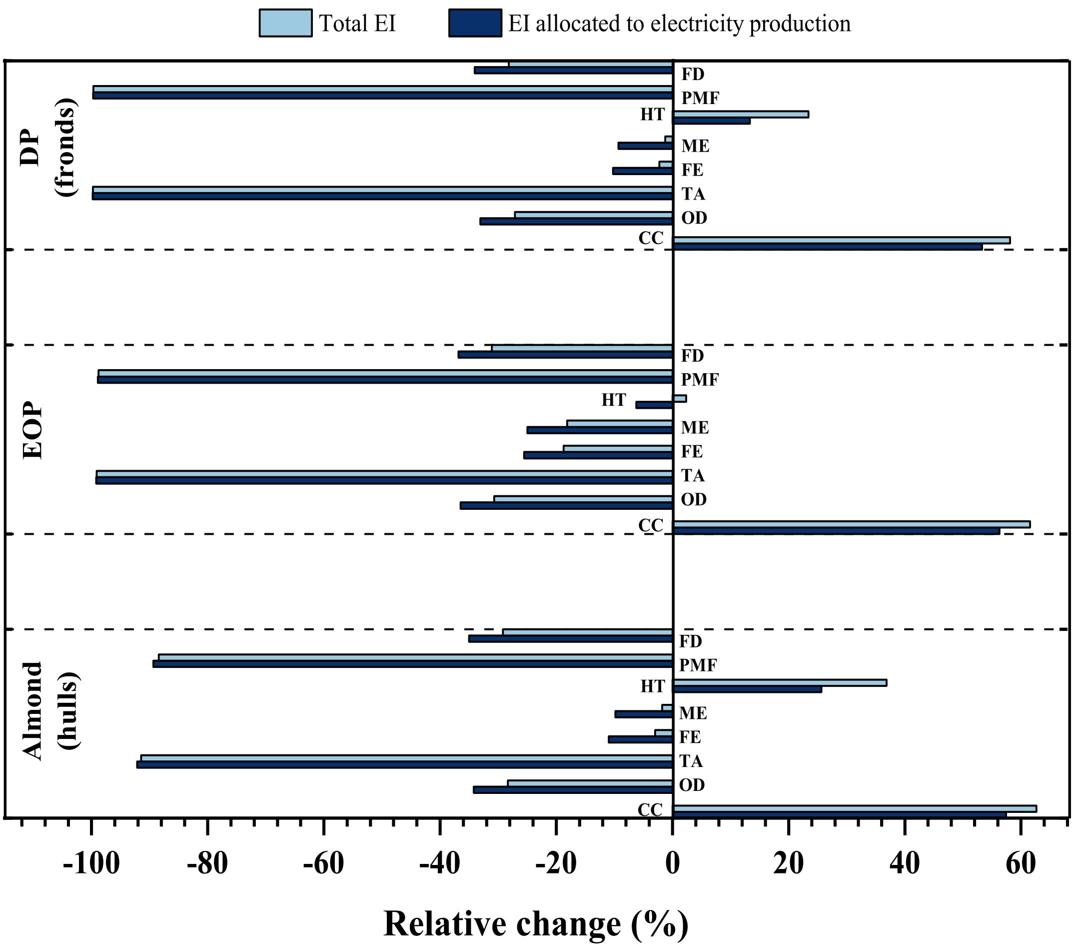

Figure 6 Comparison of environmental performance parameters for ICE and EFGT_ORC cogeneration systems, for various fuel types

5.4 Techno-economic feasibility assessment

The techno-economic feasibility is assessed and compared in this section of both cogeneration systems using two waste heat recovery technologies: cogeneration with ICE and cogeneration with EFGT-ORC. The considerations and assumptions made for the economic assessment follow:

• The cogeneration system operates for 7,500 hours yearly and only requires two monthly shutdowns for maintenance work [45]. The operational lifespan of the cogeneration plant for the economic feasibility assessment is estimated at 20 years [45].

• The capital expenditure required for the downdraft gasifier in the present work is estimated through the following expression:

$$C = C_r \left(\frac{S}{S_r}\right)^m \tag{13}$$

where C_r is the investment cost for a reference plant with a capacity S_r, C the investment cost for a plant with similar characteristics but a different capacity S, and m is the scaling factor, which takes values within the range of 0.5–1 and typically assumed to be 0.7 in the context of gasification systems [32]. The cost of the gasification technology for CHP applications was obtained directly from a manufacturer, which indicated that the capital investment required for a downdraft gasifier and producer gas conditioning unit with a rated consumption of 607 kg/h of olive pomace pellets is approximately $375,000. With the above considerations, the cost of gasification systems of varying capacity can be estimated through Eq. (13). In the simulated cogeneration plant equipped with EFGT_ORC, the cost of the downdraft gasifier was estimated to constitute 95% of the total investment, indicating that the gas conditioning unit accounts for the remaining 5% [46].

• In the cogeneration system equipped with ICE as a power generation unit, the power capital cost of the ICE was presumed to be $695.04/kW$_e$ based on a 100 kW$_e$ ICE, as reported by Wu et al. [47]. This estimation was further validated with data provided by the manufacturer, applying Eq. (13) to an ICE of different size running on producer gas.

On the other hand, the cost of the heat exchanger for hot water production was determined through the following empirical equation:

$$C_{\mathrm{HX}} = 12000\left(\frac{A_{\mathrm{HX}}}{100}\right)^{0.6} \tag{14}$$

where C_{HX} represents the cost of the heat exchanger in US dollars, while A_{HX} denotes its area in square meters [24].

• The capital cost of the ORC was estimated by aggregating the costs of its individual components using the empirical correlations in Table 11. According to these correlations, the power capital cost of the ORC amounts to approximately \$4320/kW$_e$. For context, Pantaleo et al. [48] conducted a thermoeconomic optimization study focused on small-scale organic Rankine cycle systems for waste heat recovery applications. They performed a screening of 18 organic working fluids and reported power capital costs in the range of \$2000–5000/kW$_e$. Spale et al. [49] documented a capital expenditure of €34,056 for a biomass-fired ORC unit with 6.2 kW$_e$, resulting in a power capital cost of roughly €5500/kW$_e$. It is worth noting that the power capital cost of an ORC unit tends to decrease with higher electrical power output [50]. For systems with relatively low electrical power output (<50 kW$_e$), the power capital cost typically exceeds €3000/kW$_e$ [50].

• The capital cost of the EGFT unit was estimated through the empirical correlation provided by Roy et al. [51], resulting in a power capital cost of €880.51/kW$_e$. This assessment was further reinforced by comparison with the findings of Camporeale et al. [52], who reported a capital cost of €1,200,000 for an EFGT with a rated electrical power output of 1383 kW$_e$. This is equivalent to a power capital cost of €867.68/kW$_e$.

• The operational and maintenance expenses were estimated at \$0.01/kWh. Similarly, Vera et al. [34] observed slightly lower operational and maintenance costs, amounting to

€0.007/kWh, for a biomass gasification plant equipped with a downdraft gasifier fueled by olive industry wastes and an ICE with a rated power of 70 kW_e as power generation unit.

• The fixed and installation costs of the gasification plant (civil works, electrical and mechanical assemblies) are estimated as 20% of the total investment.

• In addition to the renewable electricity generation, the simulated cogeneration plants produce heat. The thermal energy is sold at a price of $10/$MWh_{th}$, which is a competitive price when compared to the market prices of fuels for domestic uses in Tunisia in 2024 (approximately $30/$MWh_{th}$ for natural gas and $70/$MWh_{th}$ for diesel fuel) [42, 43].

• The annual discount rate was assumed equal to 8% based on the prevailing interest rates observed in Tunisia during 2024 [44].

Table 11 Purchase cost correlations of ORC equipment. All costs are expressed in US dollars

Equipment	**Cost correlation**	**Source**
Condenser	$C_{condenser} = 1773 \times \dot{m}_{\mathrm{ORC}}$	[53]
Pump	$C_{pump} = 3540 \times (P_{pump})^{0.71}$	[53]
Evaporator	$C_{evaporator} = 8500 + 409 \times A^{0.85}$	[53]
Expander	$C_{expander} = 6000 \times (P_{expander})^{0.7}$	[54]
Generator	$C_{generator} = 60 \times (P_{gen})^{0.95}$	[55]
Regenerator	$C_{regenerator} = 8500 + 409 \times A^{0.85}$	[53]

Table 12 reports the results from the economic feasibility assessment of both cogeneration systems. The evaluation includes three types of biomass feedstock: almond hull, EOP, and DP fronds. Focusing on the SPB and DPB, it is evident that the cogeneration with ICE generally exhibits shorter payback periods compared to the EFGT-ORC technology for all biomass feedstocks. This suggests a faster return on investment with the ICE technology, with the SPB ranging from 3.70 to 3.9 years and DPB varying from 4.6 to 4.9 years depending on the choice of biomass feedstock. Considering the NPV, profitability index and IRR, higher values indicate more favorable economic returns during the 20-year useful lifespan of the cogeneration plant. In this case, the NPV, PI and IRR are generally higher for cogeneration with ICE across all biomass feedstocks compared to cogeneration with EFGT-ORC. However, the differences in NPV, PI and IRR values between the two technologies are relatively small. Nevertheless, cogeneration with ICE generally exhibits higher LCOE values compared to cogeneration with EFGT-ORC for all biomass feedstocks, suggesting that EFGT-ORC technology may offer slightly lower electricity production costs.

Regarding the differences between biomass feedstocks, it is noted that each feedstock has unique characteristics such as energy content, availability, and cost. In this case, the results show some variation in economic indicators for various biomass feedstocks. Almond hulls generally result in shorter payback periods, and higher NPV, PI and IRR compared to EOP and DP fronds for both cogeneration technologies, mostly due to their lower price and relatively low consumption. EOP biomass tends to show slightly longer payback periods, lower NPV, PI and IRR compared to the almond hulls and DP biomass feedstocks, despite having lowest feedstock consumption, mostly because of its higher price. Date palm fronds exhibit competitive economic performance across most indicators, falling between almond and olive biomass in terms of economic feasibility. Although almond hulls apparently show slightly better economic metrics, the comparatively larger production and availability of olive pomace biomass in Tunisia suggest it may hold greater potential, despite its higher cost [22]. Nevertheless, due to its relatively high impact, the effect of the biomass cost on the economic performance is assessed and discussed in the next section.

Table 12 Results of economic feasibility assessment of the cogeneration systems

Financial appraisal indicator	Cogeneration with ICE			Cogeneration with EFGT-ORC		
	Almond (hulls)	**EOP**	**DP (fronds)**	**Almond (hulls)**	**EOP**	**DP (fronds)**
SPB (years)	3.70	3.97	3.87	4.17	4.35	4.32
DPB (years)	4.57	4.97	4.81	5.28	5.57	5.51
NPV (k$)	372	314	368	344	310	337
PI	1.65	1.47	1.54	1.35	1.25	1.27
IRR (%)	26.77	24.86	25.60	23.63	22.55	22.78
LCOE ($/kWh)	0.0618	0.0696	0.0623	0.0564	0.0608	0.0573

5.5 Techno-economic sensitivity assessment

Figure 7 examines the sensitivity of variations in the purchase price of biomass feedstock, electricity sale price, and heat sale price on key financial metrics of both cogeneration systems fueled with EOP. These metrics include the return on investment, assessed through the discounted payback period, as well as the profitability index and internal rate of return.

The most influential variables for both simulated cogeneration systems are the biomass price and the electricity price. For the cogeneration system with ICE, the biomass price has a stronger effect, since it requires a higher feedstock consumption than the cogeneration system with EFGT-ORC to produce the same electric power output. In fact, if the biomass feedstock purchase price is higher than $0.06/kg in the cogeneration system with ICE, the plant becomes economically unsustainable. By contrast, the cogeneration system with EFGT-ORC can operate with a biomass purchase price up to $0.08/kg, mostly due to its lower feedstock consumption. Unlike the biomass purchase price, the electricity price has a similar effect on both systems, because the rated electric power output of both system is the same, leading to identical income streams from the sale of electricity, although dissimilar capital expenditures and slightly different expenses associated with other parameters. In both cases, the cogeneration system becomes notably appealing financially, with electricity sale prices exceeding $0.1/kWh. Finally, the heat price is the variable with the least relevant effect on the financial metrics. However, it is seen that the effect of the heat price is more important in the cogeneration system with ICE, because it produces more heat compared to the cogeneration system with EFGT-ORC.

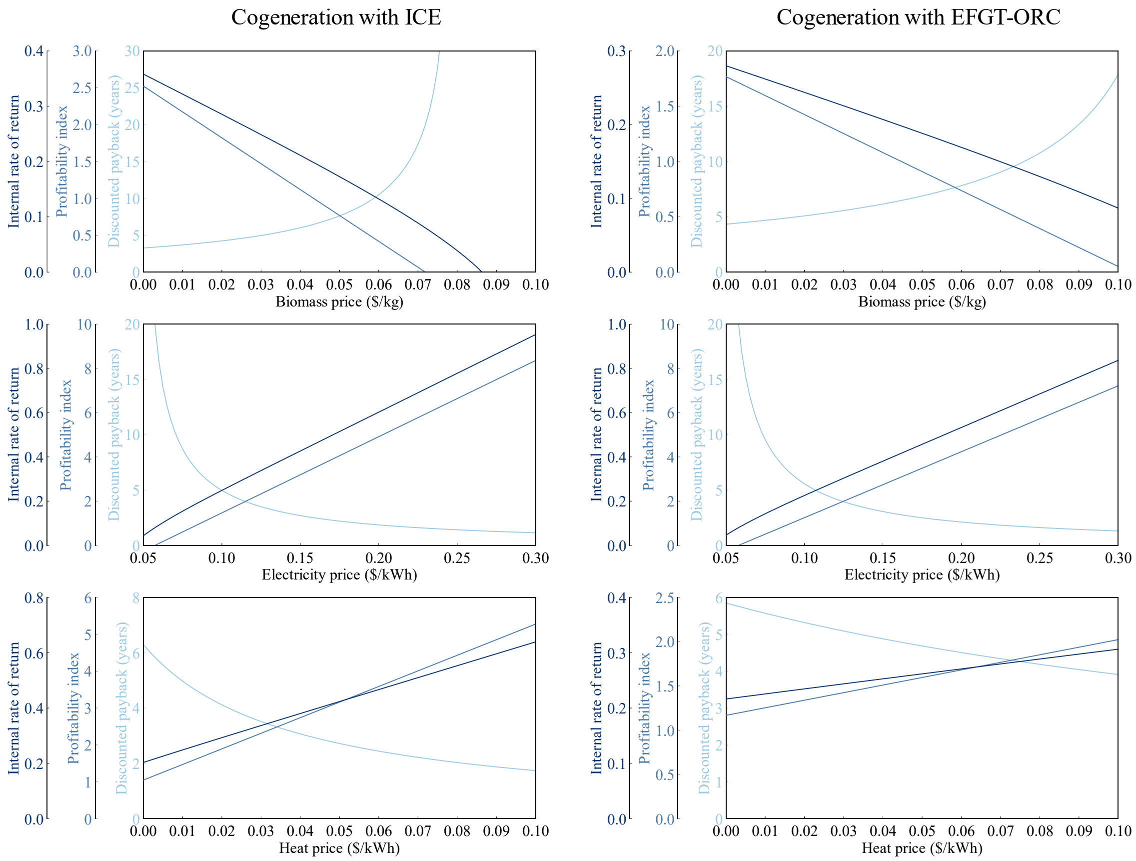

Figure 7 Sensitivity analysis for variations of the percentage of subsidy on biomass price (top), electricity price (center) and heat price (bottom).

6 Conclusion

Comprehensive evaluations of environmental impacts and techno-economic feasibility have been performed of gasification-based ICE and EFGT-ORC cogeneration systems for sustainable bioenergy production. Given their abundance, particularly in Mediterranean countries, it is suggested that these systems be fueled with agri-food residues such as almond hulls, exhausted olive pomace, and date palm fronds. Both cogeneration systems for each fuel are analyzed for energy production of 100 kJ of electricity under identical conditions.

The results from simulation of both cogeneration systems using the three biomass fuels reveal that the biomass input for EFGT_ORC is lower than for ICE, regardless of the fuel type. In ICE cogeneration, each fuel contributes about 20% to electricity and 25% to hot water, while EFGT_ORC allocates approximately 36% to electricity and 11% to hot water for all fuels. However, the energy efficiencies of both ICE cogeneration and EFGT_ORC cogeneration for almond hulls, EOP, and DP fronds fuels are found to be very similar (around 48%).

The results of LCA using midpoint and endpoint methods indicate that EFGT_ORC cogeneration has higher environmental impacts in terms of TA, PMF, and FD than ICE, for all fuels considered. Additionally, DP fronds as a fuel exhibit more significant impacts compared to almond hulls and EOP in EFGT_ORC cogeneration. The LCA also reveal that the environmental impacts of using almond hulls, EOP, and DP fronds fuels in the ICE cogeneration cycle are less significant in terms of resource depletion compared to the EFGT_ORC cogeneration. The developed midpoint environmental impact results for ICE cogeneration, compared to the EFGT_ORC system for all three evaluated biomass fuels, also show that, except for HT and CC impacts, the remaining midpoint impacts demonstrate a decrease in environmental effects for the ICE cogeneration relative to the EFGT_ORC system.

The findings of the technoeconomic analysis reveal that cogeneration with ICE offers shorter payback periods compared to EFGT-ORC technology. This translates into quicker returns on investment, with SPB ranging from 3.70 to 3.97 years and DPB from 4.57 to 4.97 years. Higher NPV, PI, and IRR values over the 20-year period favor cogeneration with ICE, despite minor differences compared to EFGT-ORC. However, cogeneration with ICE tends to have higher LCOE values, indicating that EFGT-ORC may offer slightly lower electricity production costs. Almond hulls demonstrate superior economic performance with shorter payback periods and higher NPV, PI, and IRR compared to EOP and DP fronds, attributed to their lower price and consumption, while EOP and DP fronds exhibit competitive economic feasibility, with olive pomace biomass holding greater potential despite its higher cost. The sensitivity analysis illustrates that variations in biomass feedstock purchase price, electricity sale price, and heat sale price significantly impact key financial metrics of cogeneration systems fueled with EOP, with biomass price and electricity price being the most influential variables, notably affecting the economic sustainability of the systems.

References

[1] Kataya G, Cornu D, Bechelany M, Hijazi A, Issa M. Biomass Waste Conversion Technologies and Its Application for Sustainable Environmental Development—A Review. Agronomy 2023; 13(11): 2833.

[2] Ezeorba TP, Okeke ES, Mayel MH, Nwuche CO, Ezike TC. Recent advances in biotechnological valorization of agro-food wastes (AFW): Optimizing integrated approaches for sustainable biorefinery and circular bioeconomy. Bioresource Technology Reports 2024:101823.

[3] Alagumalai A, Anvari S, Awad MM. Water: a global grand challenge and a path forward. In Solar-driven water treatment 2022 (pp. 1-35). Academic Press.

[4] Ribeiro GF, Junior AB. The global energy matrix and use of agricultural residues for bioenergy production: A review with inspiring insights that aim to contribute to deliver solutions for society and industrial sectors through suggestions for future research. Waste Management & Research 2023; 41(8): 1283-304.

[5] Anvari S, Khalilarya S, Zare V. Power generation enhancement in a biomass-based combined cycle using solar energy: thermodynamic and environmental analysis. Applied Thermal Engineering 2019; 153: 128-41.

[6] Raheem A, He Q, Ding L, Dastyar W, Yu G. Evaluating performance of pyrolysis and gasification processes of agriculture residues-derived hydrochar: Effect of hydrothermal carbonization. Journal of Cleaner Production 2022; 338: 130578.

[7] Indrawan N, Kumar A, Moliere M, Sallam KA, Huhnke RL. Distributed power generation via gasification of biomass and municipal solid waste: A review. Journal of the Energy Institute 2020; 93(6): 2293-313.

[8] Tabriz ZH, Khani L, Mohammadpourfard M, Akkurt GG. Biomass driven polygeneration systems: A review of recent progress and future prospects. Process Safety and Environmental Protection 2023; 169: 363-97.

[9] Susastriawan AA, Purwanto Y, Purnomo. Biomass gasifier–internal combustion engine system: review of literature. International Journal of Sustainable Engineering 2021; 14(5): 1090-100.

[10] Rovas D, Zabaniotou A. Exergy analysis of a small gasification-ICE integrated system for CHP production fueled with Mediterranean agro-food processing wastes: The SMARt-CHP. Renewable Energy 2015; 83: 510-7.

[11] Anvari S, Szlęk A, Arteconi A, Desideri U, Rosen MA. Comparative study of steam injection modes for a proposed biomass-driven cogeneration cycle: Performance improvement and CO2 emission reduction. Applied Energy 2023; 329: 120255.

[12] González AM, Jaén RL, Lora EE. Thermodynamic assessment of the integrated gasification-power plant operating in the sawmill industry: An energy and exergy analysis. Renewable Energy 2020; 147: 1151-63.

[13] Kavathia K, Prajapati P. A review on biomass-fired CHP system using fruit and vegetable waste with regenerative organic Rankine cycle (RORC). Materials Today: Proceedings 2021; 43: 572-8.

[14] Onabanjo T. Techno-economic and environmental assessment of gas turbines utilizing biofuels. PhD Thesis. United Kingdom: Cranfield University; 2015. Available at: http://dspace.lib.cranfield.ac.uk/handle/1826/9280

[15] Klein SJ, Rubin ES. Life cycle assessment of greenhouse gas emissions, water and land use for concentrated solar power plants with different energy backup systems. Energy Policy 2013; 63: 935-50.

[16] Wunderlich J, Armstrong K, Buchner GA, Styring P, Schomäcker R. Integration of techno-economic and life cycle assessment: Defining and applying integration types for chemical technology development. Journal of Cleaner Production 2021; 287: 125021.

[17] Voultsos I, Katsourinis D, Giannopoulos D, Founti M. Integrating LCA with Process Modeling for the Energetic and Environmental Assessment of a CHP Biomass Gasification Plant: A Case Study in Thessaly, Greece. Eng. 2020; 1(1): 2.

[18] Chen J, Liu Y, Wu X, Jiaqiang E, Leng E, Zhang F, Liao G. Thermodynamic, environmental analysis and comprehensive evaluation of supercritical water gasification of biomass fermentation residue. Journal of Cleaner Production 2022; 361: 132126.

[19] Pati S, De S, Chowdhury R. Integrated techno-economic, investment risk and life cycle analysis of Indian lignocellulosic biomass valorisation via co-gasification and syngas fermentation. Journal of Cleaner Production 2023; 423: 138744.

[20] Chen Y, Hua H, Xu J, Yun Z, Wang J, Lund PD. Techno-economic cost assessment of a combined cooling heating and power system coupled to organic Rankine cycle with life cycle method. Energy 2022; 239: 121939.

[21] Zang G, Zhang J, Ratner A, Shi Y. Techno-economic analysis of a cooling, heating, and electricity trigeneration system based on downdraft fixed bed wood and tire gasification: Case study of a campus office building. Sustainable Energy Technologies and Assessments 2023; 55: 102939.

[22] Anvari S, Aguado R, Jurado F, Fendri M, Zaier H, Larbi A, Vera D. Analysis of agricultural waste/byproduct biomass potential for bioenergy: The case of Tunisia. Energy for Sustainable Development 2024; 78: 101367.

[23] De Mena B, Vera D, Jurado F, Ortega M. Updraft gasifier and ORC system for high ash content biomass: A modelling and simulation study. Fuel Processing Technology 2017; 156: 394-406.

[24] Anvari S, Vera D, Aguado R, Jurado F, Desideri U. Developing an off-grid biomass gasification cogeneration system for Moroccan olive oil mills: Simulation, experimental validation, and 3E analysis. Energy Conversion and Management 2023; 298: 117781.

[25] Rebitzer G, Ekvall T, Frischknecht R, Hunkeler D, Norris G, Rydberg T, Schmidt WP, Suh S, Weidema BP, Pennington DW. Life cycle assessment: Part 1: Framework, goal and scope definition, inventory analysis, and applications. Environment International 2004; 30(5): 701-20.

[26] Ramos JS, Ferreira AF. Techno-economic analysis and life cycle assessment of olive and wine industry co-products valorisation. Renewable and Sustainable Energy Reviews 2022; 155: 111929.

[27] Islam S, Ponnambalam SG, Lam HL. Review on life cycle inventory: methods, examples and applications. Journal of Cleaner Production 2016; 136: 266-78.

[28] Segura-Salazar J, Lima FM, Tavares LM. Life Cycle Assessment in the minerals industry: Current practice, harmonization efforts, and potential improvement through the integration with process simulation. Journal of Cleaner Production 2019; 232: 174-92.

[29] Pang B, Yang P, Wang Y, Kendall A, Xie H, Zhang Y. Life cycle environmental impact assessment of a bridge with different strengthening schemes. The International Journal of Life Cycle Assessment 2015; 20: 1300-11.

[30] Heijungs R, Goedkoop M, Struijs J, Effting S, Sevenster M, Huppes G. Towards a life cycle impact assessment method which comprises category indicators at the midpoint and the endpoint level. Report of the first project phase: Design of the new method VROM report, online: http://www. leidenuniv. nl/cml/ssp/publications/recipe_phase1. pdf. 2003.

[31] Fernández-Lobato L, Aguado R, Jurado F, Vera D. Biomass gasification as a key technology to reduce the environmental impact of virgin olive oil production: A life cycle assessment approach. Biomass and Bioenergy 2022; 165: 106585.

[32] Salisu J, Gao N, Quan C. Techno-economic Assessment of Co-gasification of Rice Husk and Plastic Waste as an Off-grid Power Source for Small Scale Rice Milling - an Aspen Plus Model Journal of Analytical and Applied Pyrolysis 2021: 158: 105157.

[33] Anvari S, Desideri U, Taghavifar H. Design of a combined power, heating and cooling system at sized and undersized configurations for a reference building: Technoeconomic and topological considerations in Iran and Italy. Applied Energy 2020; 258: 114105.

[34] Vera D, Jurado F, Margaritis N K, Grammelis P. Experimental and economic study of a gasification plant fuelled with olive industry wastes. Energy for Sustainable Development 2014; 23: 247–57.

[35] Remón J, Latorre-Viu J, Matharu AS, Pinilla JL, Suelves I. Analysis and optimisation of a novel 'almond-refinery' concept: Simultaneous production of biofuels and value-added chemicals by hydrothermal treatment of almond hulls. Science of The Total Environment 2021; 765: 142671.

[36] Jenkins B, Ebeling J. Thermochemical properties of biomass fuels. California Agriculture 1985; 39: 14-6.

[37] Aguado R, Escámez A, Jurado F, Vera D. Experimental assessment of a pilot-scale gasification plant fueled with olive pomace pellets for combined power, heat and biochar production. Fuel 2023; 344: 128127.

[38] Oktay Z. Olive cake as a biomass fuel for energy production. Energy Sources, Part A 2006; 28: 329–39.

[39] Younis M, Farag HA, Alhamdan A, Aboelasaad G, El-Abedein AI, Kamel RM. Utilization of palm residues for biochar production using continuous flow pyrolysis unit. Food Chemistry: X. 2023; 20: 100903.

[40] Bensidhom G, Hassen-Trabelsi AB, Alper K, Sghairoun M, Zaafouri K, Trabelsi I. Pyrolysis of Date palm waste in a fixed-bed reactor: Characterization of pyrolytic products. Bioresource Technology 2018; 247: 363-9.

[41] Huijbregts MA, Steinmann ZJ, Elshout PM, Stam G, Verones F, Vieira M, Zijp M, Hollander A, Van Zelm R. ReCiPe2016: a harmonised life cycle impact assessment method at midpoint and endpoint level. The International Journal of Life Cycle Assessment 2017; 22: 138-47.

[42] www.GlobalPetrolPrices.com, Tunisia natural gas prices, https://www.globalpetrolprices.com/Tunisia/natural_gas_prices/, accessed on April 10, 2024.

[43] www.GlobalPetrolPrices.com, Tunisia diesel prices, https://www.globalpetrolprices.com/Tunisia/diesel_prices/, accessed on April 10, 2024.

[44] Reuters, Tunisia's central bank keeps key interest rate unchanged at 8%, https://www.reuters.com/markets/rates-bonds/tunisias-central-bank-keeps-key-interest-rate-unchanged-8-2024-03-22/, accessed on April 10, 2024.

[45] Allesina G, Pedrazzi S. Barriers to success: A technical review on the limits and possible future roles of small scale gasifiers. Energies 2021; 14(20): 6711.

[46] Wang J, Mao T, Sui J, Jin H. Modeling and performance analysis of CCHP (combined cooling, heating and power) system based on co-firing of natural gas and biomass gasification gas. Energy 2015; 93: 801-15.

[47] Wu J, Wang J, Wu J, Ma C. Exergy and exergoeconomic analysis of a combined cooling, heating, and power system based on solar thermal biomass gasification. Energies 2019; 12(12): 2418.

[48] Pantaleo AM, Simpson M, Rotolo G, Distaso E, Oyewunmi OA, Sapin P, De Palma P, Markides CN. Thermoeconomic optimisation of small-scale organic Rankine cycle systems based on screw vs. piston expander maps in waste heat recovery applications. Energy Conversion and Management 2019; 200: 112053.

[49] Spale J, Vodicka V, Zeleny Z, Pavlicko J, Mascuch J, Novotny V. Scaling up a woodchip-fired containerized CHP ORC unit toward commercialization. Renewable Energy 2022; 199: 1226-36.

[50] Quoilin S, Van Den Broek M, Declaye S, Dewallef P, Lemort V. Techno-economic survey of Organic Rankine Cycle (ORC) systems. Renewable and Sustainable Energy Reviews 2013; 22: 168-86.

[51] Roy D, Samanta S, Ghosh S. Techno-economic and environmental analyses of a biomass based system employing solid oxide fuel cell, externally fired gas turbine and organic Rankine cycle. Journal of Cleaner Production 2019; 225: 36-57.

[52] Camporeale SM, Pantaleo AM, Ciliberti PD, Fortunato B. Cycle configuration analysis and techno-economic sensitivity of biomass externally fired gas turbine with bottoming ORC. Energy Conversion and Management 2015; 105: 1239-50.

[53] Roy D, Samanta S, Roy S, Smallbone A, Roskilly AP. Fuel cell integrated carbon negative power generation from biomass. Applied Energy 2023; 331: 120449.

[54] Anvari S, Taghavifar H, Parvishi A. Thermo-economical consideration of Regenerative organic Rankine cycle coupling with the absorption chiller systems

incorporated in the trigeneration system. Energy Conversion and Management 2017; 148: 317-29.

[55] Li P, Cao Q, Li J, Lin H, Wang Y, Gao G, Pei G, Jie D, Liu X. An innovative approach to recovery of fluctuating industrial exhaust heat sources using cascade Rankine cycle and two-stage accumulators. Energy 2021; 228: 120587.